

Geology, geochronology and chemical evolution of the island of Pantelleria

L. CIVETTA*, Y. CORNETTE†, G. CRISCI‡, P. Y. GILLOT†, G. ORSI* & C. S. REQUEJO§

* Dipartimento di Geofisica e Vulcanologia, Largo S. Marcellino 10, Napoli 80138, Italy

† Centre de Faibles Radioactivités, CNRS/CEA, Gif-sur-Yvette, France

‡ Dipartimento di Scienze della Terra, Castiglione Scalo, Cosenza, Italy

§ Instituto de Pesquisas Energeticas e Nucleares, IPEN C. Postal 11049, Sao Paulo, SP, Brazil



(Received 12 December 1983; accepted 18 April 1984)

Abstract – Potassium–argon dating, field relations, geochemical and strontium–isotope compositions are reported for the island of Pantelleria (Strait of Sicily, Italy). These data support the following model for the genesis and evolution through time of the volcanic system: the peralkaline rocks originated from mantle-derived parental magmas; the trachytic magma differentiated in a low pressure magma chamber by crystal–liquid fractionation. This process led to a chemically zoned magma chamber tapped at different levels by successive eruptions. During low-pressure differentiation the $^{87}\text{Sr}/^{86}\text{Sr}$ ratios of some of the most evolved Sr-poor rhyolitic magmas increased from 0.703 up to 0.708 by contamination with crustal material.

The chemical variation displayed by the products of each of the defined eruptive cycles in the last 50 000 years suggests an open system behaviour of the magma chamber which is episodically refilled by more mafic parent magma, differentiated at high rate and episodically erupted.

1. Introduction

Several recent studies on compositionally zoned silicic ash flow tuffs have drawn attention to the differentiation processes operating in shallow level magma chambers. Shaw, Smith & Hildreth (1976), Hildreth (1977, 1981), Smith (1979), Bacon *et al.* (1981), and Mahood (1981) discuss potential processes which may be important in the evolution of silicic magma chambers. They envisage that the classical model of fractional crystallization cannot explain all the features of a differentiating silicic magma and propose that pronounced compositional zonation within high SiO_2 rhyolitic magma chambers may result from 'convection-driven thermogravitational diffusion' (Shaw, Smith & Hildreth, 1976; Hildreth, 1979; Smith, 1979) and/or volatile complexing processes (Bailey & Macdonald, 1975; Mahood, 1981). Conversely Michael (1983), on the basis of re-examination of petrochemical data for high-silica ash flow tuff, claims that crystal–liquid fractionation cannot be dismissed as an important differentiation mechanism of high-silica magmas, and Sparks, Huppert & Turner (1984) propose that convective fractionation is the dominant mechanism of crystal fractionation. Relatively little is known, however, on the differentiation processes operating in Cl-rich peralkaline magma chambers and their evolution with time. The island of Pantelleria, the type locality of the rock type pantellerite (Foerstner, 1881), has been investigated by means of geological and geochronological studies (Cornette *et al.* 1982, 1983). Pantelleria is well suited for studying the mechanics and rate of magma differentiation operating in such a peralkaline system.

The main purposes of this paper are: (a) to trace the chemical evolution of the peralkaline products of Pantelleria through time, interpreting them as a periodic recording of an evolving magma chamber; (b) to study the processes operating in the magma chamber and (c) to investigate the relations, if any, between basic and silicic volcanic activity. The paper describes the detailed stratigraphic and geochronological study of Cornette *et al.* (1983) and presents geochemical, Sr-isotope and new K–Ar age determinations.

2. Analytical Methods

2.a. K–Ar dating

The analytical techniques used by C.F.R.–Gif-sur-Yvette for K–Ar dating of young volcanic rocks and minerals have been presented elsewhere (Cassignol *et al.* 1978; Gillot, 1978; Cassignol & Gillot, 1982). The range of application has been demonstrated by Gillot *et al.* (1979), Gillot & Nativel (1982), Gillot *et al.* (1982) and Cornette *et al.* (1983).

The present measurements have been done in duplicate on mineral phases (feldspar), glass or groundmass separated from the 250 to 500 millimicron fraction of the crushed rocks. K-content was measured by atomic absorption spectrometry with a typical accuracy of 1.5%. Sample weights of 2–8 g were used for the argon extraction. Initial degassing was done at room temperature in order to avoid fractionation effects. The atmospheric argon blanks of the line typically range between 0.5 and 1.5×10^{18} atoms. Mass analyses were made with a 180°, 6 cm radius mass spectrometer operated in the static mode at an accelerating potential of about 500 V. The agreement between replicated

Table 1. $^{40}\text{K}/^{40}\text{Ar}$ age determinations of Pantelleria volcanics

Sample	Location	Eruptive cycle*	Material (K %)	Rad. ^{40}Ar (%)	Rad ^{40}Ar (10^{11} at. g $^{-1}$)	Age (10^3 years)
SIC 34	Cuddia di Midda	G	K feldspar (4.30)	0.46 0.33	0.37 0.44	8.2 ± 3.6 9.7 ± 5.9
SIC 38	Contrada Sciuvechi	F	K feldspar (4.93)	0.59 0.80	0.89 0.78	17.3 ± 5.8 15.1 ± 3.8
SIC 119	Punta dell'Alca	E	Glass (3.90) K feldspar (4.90)	1.55 4.20	1.06 1.06	26.0 ± 4.0 21.0 ± 1.5
SIC 105	Punta dello Scalo	D	Groundmass (0.87)	0.80 1.26	0.26 0.25	28.0 ± 7.0 27.5 ± 4.5
SIC 104	Punta S. Leonardo	D	Groundmass (0.70)	0.24 0.48	0.19 0.22	27.0 ± 20.0 30.5 ± 13.0
SIC 103b	Cuddia del Monte	D	Groundmass (0.85)	0.56 0.57	0.24 0.32	27.0 ± 9.5 36.0 ± 13.0
SIC 73	Monte Gibebe	C	K feldspar (2.80)	1.57 0.59	0.93 0.97	31.8 ± 4.0 33.0 ± 11.0
SIC 125	Serra di Ghirlanda	C	K feldspar (3.50)	2.02 2.20	1.19 1.32	32.5 ± 3.2 35.8 ± 3.3
SIC 68	Montagna Grande	C	K feldspar (2.95)	2.83 2.81	1.05 1.09	34.1 ± 2.4 35.3 ± 2.5
SIC 76	Punta Limarsi	B	K feldspar (5.00)	2.82	2.65	50.8 ± 3.6
SIC 20	Contrada Lago	B	K feldspar (5.01)	2.89 2.96	2.61 2.46	50.0 ± 3.5 47.0 ± 3.2
SIC 111	Costa Zighidi	A	K feldspar (4.65) Groundmass (3.82)	7.30 2.70	2.85 2.54	59.0 ± 2.0 64.0 ± 5.0
SIC 120	Calla dell'Alca	A	Groundmass (1.30)	3.06 3.38	1.14 1.11	84.0 ± 5.5 82.0 ± 5.0
SIC 107	Cuddia del Cat	A	Groundmass (1.00)	2.45 2.94	1.24 1.21	120.0 ± 10.0 117.0 ± 8.0
SIC 118	Punta del Curtigliolo	A	Groundmass (0.89)	1.04 1.20	1.14 1.12	122.0 ± 21.0 119.0 ± 19.0
SIC 116	Punta di Sciaracazza	A	Groundmass (3.67)	8.38 15.04	8.39 7.93	219.0 ± 6.0 207.0 ± 5.5
SIC 117	Punta della Salina	A	Groundmass (4.05)	3.37 3.42	9.64 9.35	228.0 ± 13.0 221.0 ± 13.0

The international constants were used for age calculations (Steiger and Jager, 1977). Chemical analyses of the analysed rocks are given in Tables 2 and 3.

* Eruptive cycle letters are mentioned in the text.

determinations appears to be good and is always better than the given error which is calculated from the uncertainty in the correction for atmospheric contamination (Gillot *et al.* 1982), the major uncertainty for samples with less than 10% of radiogenic argon.

The location of the analysed samples and the results are reported in Table 1. The obtained ages are always in agreement with the stratigraphic succession and with either the available fission track ages (Bigazzi *et al.* 1971; Bigazzi, Bonadonna & Radi, 1982) or the previously published K-Ar age determinations (Cornette *et al.* 1983).

2.b. Geochemistry

Major elements, with the exception of Mg and Fe which were determined by atomic absorption spectrometry and titration respectively, were analysed by X-ray fluorescence (XRF) with full matrix effect correction (Franzini & Leoni, 1972). Rb, Sr, Ba, La, Ce, Zr, Nb and Y were analysed by XRF following the method described in Leoni & Saitta (1976). Precision for Rb,

Zr, Ba, Sr is better than $\pm 5\%$, for La, Ce, Nb, Y, V is better than $\pm 10\%$, for Sr and Ni contents lower than 10 ppm is better than $\pm 50\%$. Accuracy was monitored by international standards and is always better than 10%.

La, Ce, Eu, Tb, U, Sb, Ba, Cs, Sc, R, Hf, Rb, Ta, Co were analysed by Instrumental Neutron Activation Analysis (INAA) at the Instituto de Pesquisas Energeticas e Nucleares (Sao Paulo, Brazil). Thermal and epithermal irradiations were used for INAA. Nd, Gd, Yb and Th abundances were determined after radiochemical separation. Precision for Th, U, Hf, Ba, Sr, Rb, Ta, La, Sm, Eu, Nd, Gd is better than $\pm 10\%$ and for Ce, Yb, Lu, Tb is better than $\pm 15\%$ for the range of abundances of BCR-1 and G-2.

$^{87}\text{Sr}/^{86}\text{Sr}$ ratios were measured on a VG micromass 30 mass spectrometer at the Department of Earth Sciences, University of Leeds, England. All the isotopic data have been normalized to 0.70800 for Eimer and Amend SrCO_3 . The quoted errors on the $^{87}\text{Sr}/^{86}\text{Sr}$ ratios are the standard deviation of the mean at two sigma levels.

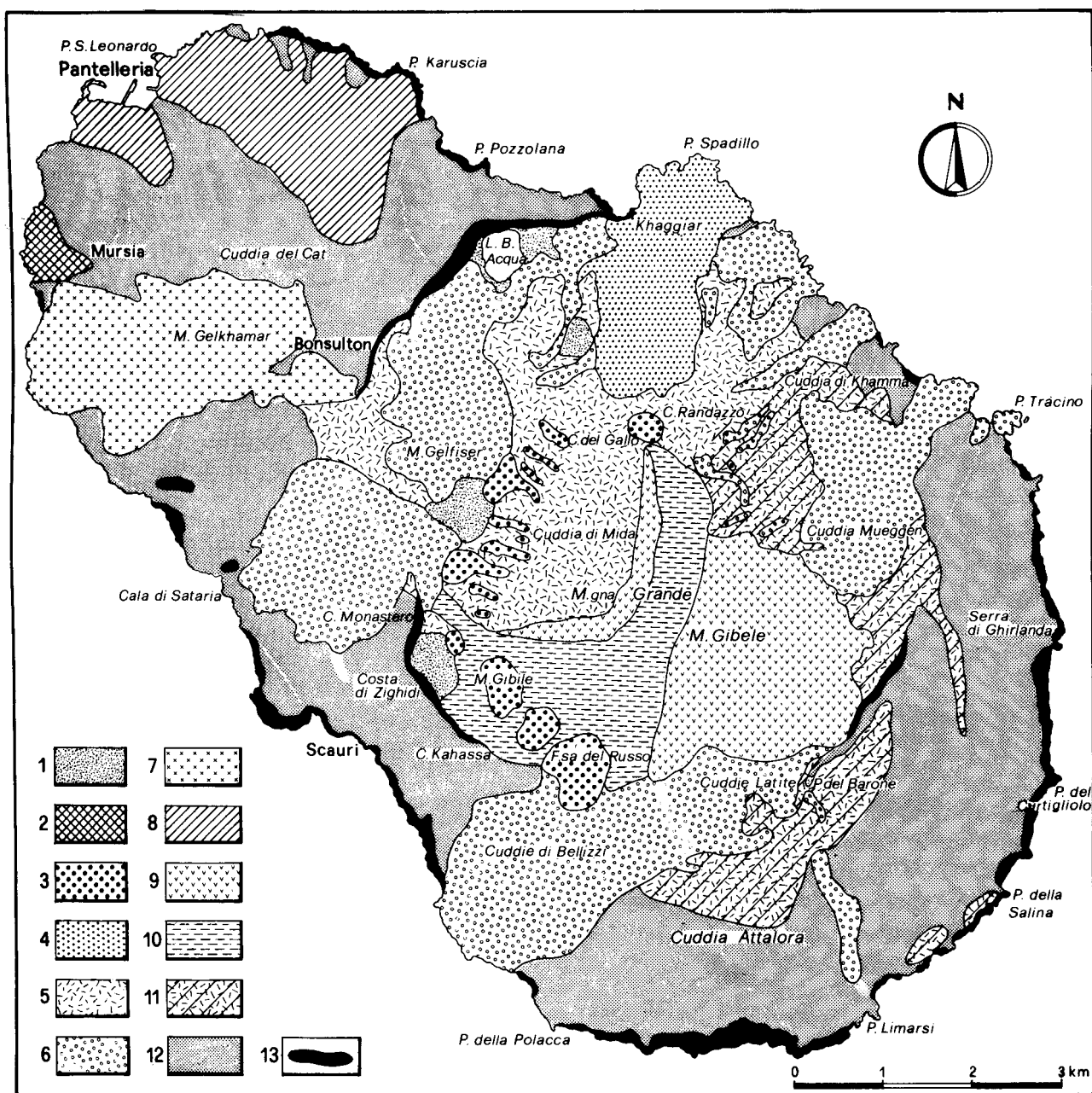


Figure 1. Lithologic map of the island of Pantelleria (modified after Villari in Rittmann, 1967). 1: Recent sedimentary deposits; 2: Mursia basaltic lava flows and cinder cones; 3: Upper pantelleritic lava flows and domes; 4: pantelleritic domes and lava flows; 5: Cuddia di Mida tephra; 6: Lower pantelleritic lava flows and domes; 7: Gelkhamar pantelleritic endogenous dome and lava flows; 8: P. San Leonardo basaltic lava flows and cinder cones; 9: Mt. Gibebe lava flows; 10: Montagna Grande dome; 11: Serra di Ghirlanda tephra; 12: green tuff; 13: volcanic units older than the green tuff.

3. Geological History

Pantelleria (Fig. 1) is located in the Pantelleria Rift which is along the deepest part of the Strait of Sicily. This rift is floored by a continental type crust which is 20 km thick in its central part and reaches 30–40 km under Sicily and Africa (Colombi *et al.* 1973; Cassinis, Franciosi & Scarascia, 1979). It is characterized by horsts and grabens formed by NW–SE tensional faults and NE–SW shear faults (Colantuoni & Zarudzski, 1973). Several faults and fractures following the

regional trends are recognizable on the island. The most significant volcano-tectonic features are: (a) two calderas of different ages and (b) the uplifting of the Montagna Grande Block (Cornette *et al.* 1982; 1983). The results of gravity and geomagnetic surveying (Agocs, 1959; Gantar *et al.* 1961; Berrino *et al.* 1984) suggest the presence of a dome-shaped intrusion of 0.003 kg/m³ under the island.

The island of Pantelleria is characterized by the occurrence of a bimodal association of basaltic and trachytic–rhyolitic volcanism, the former being largely

subordinate. Only a few rocks with SiO₂ content ranging between 54 and 62% have been found, mainly as xenoliths in the silicic units (Villari, 1974*b*; this paper). The chemistry and mineralogy of the Pantelleria volcanics has been investigated by Washington (1913–14), Zies (1960, 1962, 1966), Carmichael (1962, 1967), Rittmann (1967), Romano (1968, 1969), Noble & Haffty (1969), Villari (1970, 1974*a, b*), Korringa & Noble (1972) and Wolff & Wright (1981*b*). Cornette *et al.* (1982, 1983) have given a reconstruction of the volcanic history of the island over the last 50 000 a B.P., which greatly differs from earlier models. A summary of the geologic history (Fig. 1), integrated with new K–Ar age determinations (Table 1), follows.

The oldest dated volcanic events are the eruption of a trachytic dome and the intrusion of a trachytic dyke at 220 000 a B.P. (Table 1). These events were followed by several silicic eruptions forming a great number of flows, domes and pyroclastic deposits. This activity gave rise to different volcanic structures as deduced from the morphology and from the lack of continuity of the different units. In the southern part of the island these volcanic units attain a thickness of about 300 m in sea cliff exposures.

From 220 000 to 50 000 a B.P. there were two episodes of basaltic activity. The older is dated around 120 000 a B.P. (Table 1) and its products have been found at Cuddia del Cat cinder cone and at Punta del Curtigliolo as a dyke. The younger is dated around 80 000 a B.P. (Table 1) and formed lava flows and cinder cones outcropping at Cala dell'Alca.

The old volcanic activity was followed by the eruption of a pyroclastic sheet 50 000 a B.P. which covered all the island; the deposit forms an important stratigraphic marker. It often obscures the stratigraphy of the older products, which are only exposed on the coastal cliffs and the calderas walls. The K–Ar age of this formation of 50 000 a B.P. (Cornette *et al.* 1982, 1983) agrees with the interpolated stratigraphic age of 45 000 a B.P. (Keller *et al.* 1978, Keller, 1981) of the Y-6 ash layer in the Central Mediterranean Sea. This unit has been interpreted as an ignimbrite (Borsi *et al.* 1963; Rittmann, 1967; Villari, 1969) and as a welded air-fall tuff (Korringa, 1971; Wright, 1980; Wolff & Wright, 1981*a, b*); the non-genetic term green tuff is used. The thickness varies from a few tens of centimetres up to 20 m and the sheet covers an area of at least 85 km². The minimum volume has been estimated at 0.76 km³ dense rock equivalent (Wolff & Wright, 1981*b*). The eruption of the green tuff was followed by the collapse of the Monastero Caldera, which has been the site of most of the subsequent silicic volcanism.

After a period of quiescence, the Montagna Grande volcanic complex 35 000 a B.P. was erupted within the Monastero Caldera in at least three stages. Volcanic activity started with the eruption of the pantelleritic Serra di Ghirlanda tephra and followed with the effusion of the trachytic Montagna Grande dome. In

the later stages of the growth of this dome a summit collapse took place with the subsequent formation of the trachytic Mt. Gibeles volcanic cone. The north-western part of the Montagna Grande volcanic complex was uplifted by at least 300 m on its southeastern side at an estimated average rate of 1.5 cm/a for about 20 000 a. Fissure basaltic activity took place in the northwestern part of the island at around 30 000 a B.P. (Table 1) along NW–SE trending fractures, which align with the Pantelleria rift direction. The pantelleritic Gelkamar dome (Villari, 1968, 1974*b*) was formed at 22 000 a B.P., erupting a huge amount of pantelleritic lava flows in the later stages of its growth.

After a period of quiescence, about 16 000 years ago volcanic activity resumed with the eruption of the Lower pantelleritic lava flows and domes. Most of the vents are located on the rim of the Monastero Caldera (Fig. 1). At 9 000 a B.P. explosive eruption formed the pantelleritic pyroclastic fall deposits termed the Cuddia di Mida tephra. The main vents for this activity are Cuddia di Mida and Cuddia Randazzo. This was followed by the eruption of the Upper pantelleritic lava flows and domes. The eruption of the pantelleritic Khaggiar dome and related lava flows on the northeastern coast probably represents the youngest silicic activity on the island. Both the Gelfiser and Khaggiar domes should lie on the northern rim of the Monastero caldera.

The most recent volcanic activity on the island is represented by the Mursia basaltic lava flows and cinder cones (Fig. 1), as suggested by the existence in these rocks of a strong ²²⁶Ra excess (half-life of 1602 a) over the equilibrium concentration with ²³⁸U (L. Civetta, unpublished data). Two basic submarine eruptions are recorded. In 1831 Graham island formed 50 km northeast of Pantelleria (Washington, 1909); in 1891 an eruption took place about 7 km northwest of Pantelleria (Ricciò, 1892; Washington, 1909).

4. Petrography

4.a. Silicic rocks

Most of the eruptive cycles on Pantelleria have involved glassy and crystalline rocks and both have been sampled to provide full coverage of the compositional range. Rocks have been termed trachyte and pantellerite on the basis of composition (Macdonald, 1974).

The abundance of phenocrysts ranges from about 20 to 5% by volume in the porphyritic rocks, and is less than 5% by volume in the rocks defined as aphyric. Anorthoclase represents approximately 90–95% of the phenocrysts in the pantellerites, showing small compositional range (Chayes & Zies, 1962, 1964; Nicholls & Carmichael, 1969). The other phenocrysts are clinopyroxene (sodic ferrohedenbergite – Carmichael, 1962; Nicholls & Carmichael, 1969), olivine (fayalite – Carmichael, 1962; Nicholls & Carmichael, 1969), aenigmatite or Fe–Ti oxides. Aenigmatite appears

Table 2. Chemical analyses of silicic rocks from *Pantelleria*

Sample no.... Eruptive cycle* Field occurrence† Porphyritic (p) or aphyric (a)	Old volcanics														
	114	116	117	74	80	77	46	44	36	27	26	25	24	23	8
SiO ₂ (%)	67.26	66.18	66.46	70.95	67.85	67.72	68.88	68.58	68.00	70.84	67.25	67.06	66.13	67.04	67.94
TiO ₂ (%)	0.69	0.66	0.72	0.44	0.62	0.61	0.53	0.59	0.61	0.53	0.69	0.65	0.72	0.55	0.66
Al ₂ O ₃ (%)	10.80	10.39	12.43	10.98	10.91	10.96	13.02	12.01	10.64	11.19	11.19	11.88	9.66	14.73	11.38
Fe ₂ O ₃ (%)	6.37	4.78	4.91	1.98	6.81	4.37	3.04	2.52	4.56	3.58	7.99	5.95	5.90	2.56	5.45
FeO (%)	3.19	4.60	3.56	3.97	2.14	4.11	2.47	3.57	3.62	2.90	1.74	3.19	4.38	2.37	3.34
MnO (%)	0.34	0.36	0.34	0.23	0.24	0.29	0.21	0.25	0.29	0.27	0.35	0.33	0.39	0.21	0.21
MgO (%)	0.63	0.41	0.60	0.17	0.42	0.16	0.55	0.46	0.38	0.45	0.31	0.53	0.29	0.53	0.88
CaO (%)	0.60	0.58	0.69	0.38	0.59	0.46	0.81	0.81	0.96	0.61	0.84	1.02	0.90	1.09	0.86
Na ₂ O (%)	5.41	6.90	5.37	5.84	5.82	6.75	5.58	6.04	5.73	4.79	4.86	4.55	6.83	6.22	4.58
K ₂ O (%)	4.29	4.17	4.66	4.27	4.17	4.24	4.55	4.49	4.39	4.42	4.44	4.51	4.25	4.32	4.37
P ₂ O ₅ (%)	0.03	0.03	0.04	0.01	0.03	0.02	0.05	0.05	0.05	0.03	0.04	0.04	0.04	0.08	0.05
Σ trace element oxides (%)	0.27	0.25	0.19	0.38	0.27	0.27	0.29	0.31	0.35	0.35	0.27	0.26	0.29	0.29	0.27
Cl %	0.16	0.87	0.06	0.51	0.18	0.04	0.03	0.43	0.54	0.06	0.04	0.02	0.27	0.02	0.01
H ₃ O ⁺ (%)	2.11	2.20	1.88	0.92	2.23	0.77	0.29	0.30	0.72	0.66	1.25	1.26	0.69	1.35	1.35
Agpaitic index	1.25	1.52	1.12	1.30	1.29	1.15	1.09	1.23	1.33	1.13	1.14	1.16	1.64	1.01	1.08
La (ppm)	152	147	111	189	148	149	132	137	172	180	146	151	152	109	146
Ce (ppm)	268	258	191	332	264	258	228	247	301	304	262	257	270	185	256
Rb (ppm)	107	103	103	154	97	108	115	121	142	113	106	98	130	82	86
Y (ppm)	107	97	78	124	101	100	87	98	130	130	102	115	112	83	104
Zr (ppm)	1142	1044	786	1699	1132	1137	1217	1294	1530	1553	1115	1034	1256	877	1169
Nb (ppm)	236	213	174	314	226	225	246	267	301	303	233	217	254	180	239
Ba (ppm)	43	27	51	26	33	43	178	142	101	68	61	66	42	695	43
Sr (ppm)	11	5	6	4	12	4	11	10	3	12	12	15	n.m.	68	15

Table 2 (continued)

Sample no. Eruptive cycle* Field occurrence† Porphyritic (p) or aphyric (a)	Green tuff				Montagna Grande volcanic complex				Gelkhamar dome												
	97	20	6	76	71	70	73	68	33	35	29	125	94	76	71	70	73	68	33	35	29
	B, e v a	B, e v a	B, l i p	B, l i p	C, e fa a	C, e fa a	C, l fl p	C, l fl p	C, l fl p	E, e d p	E, l fl p	C, e fa a	B, l i p	B, l i p	C, e fa a	C, e fa a	C, l fl p	C, l fl p	C, l fl p	E, e d p	E, l fl p
SiO ₂ (%)	69.68	68.62	67.98	66.82	71.25	71.15	65.65	62.22	62.45	68.20	—	71.25	64.48	66.82	71.15	70.57	65.65	62.22	62.45	68.20	—
TiO ₂ (%)	0.55	0.56	0.60	0.61	0.41	0.40	0.70	0.63	1.21	0.56	—	0.41	0.80	0.61	0.40	0.41	0.70	0.63	1.21	0.56	—
Al ₂ O ₃ (%)	9.32	9.65	12.63	13.24	8.17	8.12	16.14	16.39	15.46	10.53	11.88	8.17	15.50	13.24	8.12	7.96	16.14	16.39	15.46	10.53	—
Fe ₂ O ₃ (%)	6.60	5.99	3.19	2.91	4.98	4.28	3.66	2.09	3.50	4.06	—	4.98	3.07	2.91	4.28	3.66	1.28	2.09	3.50	4.06	—
FeO (%)	2.16	2.71	2.71	3.87	3.95	4.48	5.03	2.49	2.81	4.04	—	3.95	3.03	3.87	4.48	5.03	3.55	2.49	2.81	4.04	—
MnO (%)	0.28	0.29	0.23	0.26	0.28	0.22	0.19	0.15	0.19	0.26	0.25	0.28	0.21	0.26	0.22	0.27	0.19	0.15	0.19	0.26	—
MgO (%)	0.15	0.24	0.51	0.28	0.20	0.10	0.62	0.58	1.23	0.30	—	0.20	0.36	0.28	0.10	0.62	0.64	0.58	1.23	0.30	—
CaO (%)	0.38	0.89	1.05	0.70	0.34	0.39	0.35	1.61	2.40	0.94	—	0.34	1.06	0.70	0.39	0.35	0.79	1.61	2.40	0.94	—
Na ₂ O (%)	5.96	5.84	6.02	6.38	5.07	5.53	6.57	6.61	3.67	5.90	5.10	5.07	6.86	6.38	5.53	5.78	6.57	6.61	3.67	5.90	—
K ₂ O (%)	4.11	4.28	4.43	4.32	4.35	4.22	3.95	3.81	4.40	4.40	4.65	4.35	4.18	4.32	4.22	4.19	3.95	3.81	4.40	4.40	—
P ₂ O ₅ (%)	0.01	0.03	0.06	0.06	0.01	0.01	0.28	0.15	0.35	0.03	—	0.01	0.15	0.06	0.01	0.01	0.28	0.15	0.35	0.03	—
Σ trace element oxides (%)	0.38	0.41	0.31	0.23	0.50	0.50	0.26	0.27	0.27	0.42	0.35	0.50	0.29	0.23	0.50	0.52	0.26	0.27	0.27	0.42	—
Cl (%)	0.53	0.65	0.36	0.41	0.64	0.77	0.81	0.01	0.13	0.45	0.03	0.64	0.01	0.41	0.77	0.81	0.01	0.01	0.13	0.45	—
H ₂ O ⁺ (%)	0.80	0.55	1.03	1.39	4.40	3.33	4.08	0.37	0.54	0.61	0.87	4.40	0.60	1.39	3.33	4.08	0.28	0.37	0.54	0.61	—
Agpatitic index	1.56	1.46	1.16	1.15	1.60	1.68	0.93	0.91	1.07	1.37	1.13	1.60	1.06	1.15	1.68	1.76	0.93	0.91	1.07	1.37	—
La (ppm)	200	199	143	115	286	288	84	79	72	209	193	286	49	115	288	291	84	79	72	209	—
Ce (ppm)	347	246	248	193	472	476	143	133	126	367	327	472	87	193	476	483	143	133	126	367	—
Rb (ppm)	148	159	128	81	201	191	63	57	63	168	136	201	38	81	191	198	63	57	63	168	—
Y (ppm)	139	151	96	78	179	179	48	54	53	146	123	179	26	78	179	187	48	54	53	146	—
Zr (ppm)	1660	1761	1292	787	2129	2160	605	571	516	1858	1472	2129	303	787	2160	2277	605	571	516	1858	—
Nb (ppm)	314	334	246	165	405	406	130	117	170	357	305	405	73	165	406	424	130	117	170	357	—
Ba (ppm)	87	84	208	404	65	52	895	1011	1001	75	89	65	1825	404	52	37	895	1011	1001	75	—
Sr (ppm)	4	2	26	12	9	5	166	194	165	4	11	9	48	12	5	3	166	194	165	4	—

Table 3. Chemical analyses of basic and intermediate rocks from Pantelleria

Sample no....	118	3	98B	7	15	16	17a	47	48	51	9	11	52
Eruptive cycle	A	A	A	D	D	D	D	D	L	L	fl	x	x
Field occurrence	dy	fl	fl	fl	fl	fl	fl	fl	fl	fl	fl	x	x
SiO ₂ (%)	46.21	47.63	45.45	47.59	47.33	47.57	47.96	47.51	48.09	48.08	51.11	56.90	57.15
TiO ₂ (%)	3.93	3.25	3.20	2.89	2.52	2.59	2.70	2.48	2.81	3.05	2.97	1.68	1.74
Al ₂ O ₃ (%)	15.77	16.10	15.83	16.85	17.74	17.42	16.86	17.47	16.70	16.94	17.43	16.0	15.81
Fe ₂ O ₃ (%)	2.01	2.83	2.50	4.45	6.39	2.74	7.35	3.69	4.33	6.42	4.63	4.72	4.47
FeO (%)	9.81	7.02	7.93	6.62	4.31	6.56	3.33	6.20	6.54	5.18	5.77	2.58	3.06
MnO (%)	0.20	0.19	0.17	0.18	0.17	0.18	0.20	0.18	0.20	0.20	0.22	0.20	0.19
MgO (%)	5.75	6.51	7.91	6.21	6.31	6.34	5.85	6.55	5.87	4.35	4.12	3.58	3.40
CaO (%)	10.24	10.09	10.75	10.06	10.76	11.64	10.44	10.78	10.06	10.60	6.62	4.92	5.12
Na ₂ O (%)	3.69	3.75	3.72	3.28	3.03	3.20	3.44	3.44	3.61	3.47	3.89	5.64	5.38
K ₂ O (%)	1.04	1.11	1.32	0.90	0.76	0.96	0.97	0.91	0.94	0.90	0.92	2.96	2.91
P ₂ O ₅ (%)	1.54	1.21	0.92	0.74	0.46	0.54	0.68	0.55	0.65	0.59	0.99	0.51	0.49
Σ trace element oxides (%)	0.22	0.25	0.19	0.20	0.16	0.21	0.19	0.19	0.20	0.19	0.28	0.25	0.25
Cl (%)	0.11	0.06	0.15	0.03	0.08	0.06	0.05	0.06	0.03	0.05	0.06	0.08	0.04
H ₂ O ⁺ (%)	0.31	0.12	0.31	0.06	0.15	0.20	0.08	0.15	0.56	0.66	0.38	0.15	0.28
La (ppm)	40	44	65	30	20	31	28	26	31	27	80	67	63
Ce (ppm)	78	91	107	53	37	54	49	48	60	45	127	106	107
Rb (ppm)	14	22	22	16	14	18	17	17	33	14	32	44	45
Y (ppm)	29	32	28	26	23	24	27	23	27	25	36	42	40
Zr (ppm)	151	198	290	136	131	137	149	126	151	138	297	391	403
Nb (ppm)	39	41	58	30	27	18	31	31	33	29	70	85	87
Ba (ppm)	475	693	509	448	239	502	364	416	319	357	670	839	876
Sr (ppm)	479	543	710	473	474	521	466	509	462	430	642	349	340
Ni (ppm)	23	69	98	54	57	68	30	64	28	55	6	26	28
V (ppm)	363	294	299	310	270	287	291	260	319	327	229	77	81

A = old volcanics; D = Punta San Leonardo basaltic lava flows and cinder cones dated at 29000 a.; L = Mursia basaltic lava flows younger than 10000 a B.P.; x = xenoliths in silicic formations; fl = lava flow; dy = dyke.

All the numbers are preceded by SIC.

only in the pantellerites with SiO_2 concentration higher than 67%. Analyses of aenigmatite are reported by Carmichael (1962), Zies (1966) and Nicholls & Carmichael (1969). Quartz appears only in the most silicic rocks. The groundmass is generally glassy; when crystalline it consists mainly of sanidine, aegirine, amphibole, Fe–Ti oxides, quartz and apatite. The trachytes show a mineral assemblage similar to the pantellerites, the most relevant feature being the absence of aenigmatite. Anorthoclase is the most abundant phenocryst. It frequently shows distinct oligoclase cores (Villari, 1974*a*). The other phenocrysts are: clinopyroxene, fayalite, Fe–Ti oxides. The groundmass consists of alkali feldspars, Fe–Ti oxides, clinopyroxene and apatite.

4.b. Mafic rocks

The analysed mafic rocks are transitional basalts, hawaiites and mugearites. All are strongly porphyritic, containing phenocrysts of zoned plagioclase, olivine and clinopyroxene. Pyroxene phenocrysts from a hawaiite dyke are aluminous titanite; titaniferous magnetite occurs in the same rock (Bryan, 1970). The groundmass consists of plagioclase, olivine, augite, ilmenite, magnetite and apatite. Sample SIC 9 is a mugearite collected from a post-green tuff lava flow at le Balate. This flow is undated and, lacking field relationships, cannot be ascribed to any of the individual basic volcanic cycles. The rock is less porphyritic and is characterized by a more sodic plagioclase and less abundant olivine. Samples SIC 11 and SIC 52 are two strongly porphyritic xenoliths of benmoreitic composition collected in the trachytic products of Montagna Grande volcanic complex. The phenocrysts are oligoclase, clinopyroxene, olivine and rare magnetite and ilmenite.

5. Geochemistry

5.a. Major elements

In Tables 2 and 3 respectively, silicic and mafic samples belonging to the same eruptive cycle have been grouped together. For each cycle samples are listed in order of decreasing age. Location of each sample is reported in Figure 2.

In any treatment of the geochemistry of glassy silicic rocks, the possible effects of hydration and devitrification must be considered. The low values of ignition loss ($\text{H}_2\text{O}^+ < 1.0\%$) for most of the analysed silicic rocks, the coherent behaviour of the mobile elements with Zr which is considered to be extremely resistant to hydration (Pearce & Cann, 1973), indicate that this process has not significantly affected the analysed rocks. Most the analysed welded pyroclastic silicic rocks show evidence of a vapour phase crystallization. Chemical effects can be assessed using the green tuff, where such crystallization is particularly well developed

(McCormick & Sheridan, 1983). The green tuff displays a compositional vertical zonation from a strongly peralkaline first erupted portion to a trachytic last erupted part. Similar compositional trends are observed within each subsequent eruptive group (see later discussion). The occurrence of similar geochemical trends, the coherent geochemical pattern displayed by all the major and trace elements of the green tuff analysed samples and the enrichment in the samples collected from the basal vitrophyre in elements (such as the REE) which are characterized by high vapour/liquid partition coefficients (Flynn & Burnham, 1978), suggest that important chemical mobilization during vapour phase crystallization has not affected the studied green tuff samples. We thus have no evidence for significant chemical changes resulting from secondary processes.

The volcanics erupted between 220000 and 50000 a B.P. are referred to as Group A in Tables 2 and 3. They are mainly pantellerites and trachytes; basalts and hawaiites are subordinate. Chemical analyses of rocks belonging to this group are reported in Korrington & Noble (1972) and Villari (1974*b*). Variations in chemical composition with time, if any, cannot be inferred for this group. Due to the paucity of stratigraphic and geochronological data only few samples have been analysed in order to compare the bulk chemical composition of this group with that of the more recent eruptive cycles. The main chemical features of the silicic rocks are the variation of SiO_2 values from 66 to 70% with related decrease of Al_2O_3 , TiO_2 , P_2O_5 , MgO and CaO (Villari, 1974*b*).

The Group B data in Table 2 are samples from different outcrops of the green tuff. Specimens SIC 97 and SIC 20 are non-hydrated glass from the basal vitrophyre while SIC 6, SIC 76 and SIC 94 represent uppermost crystal-rich layers. Sample SIC 94 is of particular interest, representing by far the least differentiated rock yet recorded for the unit. The green tuff varies in composition from pantelleritic to trachytic from the base upwards. Chemical analyses, recalculated on anhydrous basis, show an upwards increase in Al_2O_3 , P_2O_5 , CaO, MgO and TiO_2 , a decrease in SiO_2 and a slight decrease in Na_2O . This implies the existence of a compositionally zoned magma chamber tapped at different levels during the eruption. A similar conclusion has been reported by Wolff & Wright (1981*b*) on the basis of mineralogical data.

The samples of Group C in Table 2 are from the Montagna Grande volcanic complex. Samples SIC 125, SIC 71 and SIC 70 belong to the stratigraphically lowest air-fall unit (Serra di Ghirlanda Tephra) and samples SIC 73, SIC 68 and SIC 33 are collected from Monte Gibeles lava flows. This group shows a compositional gap between the first-erupted pantellerites and the later trachytes. The Serra di Ghirlanda tephra samples are the only analysed rocks which have been

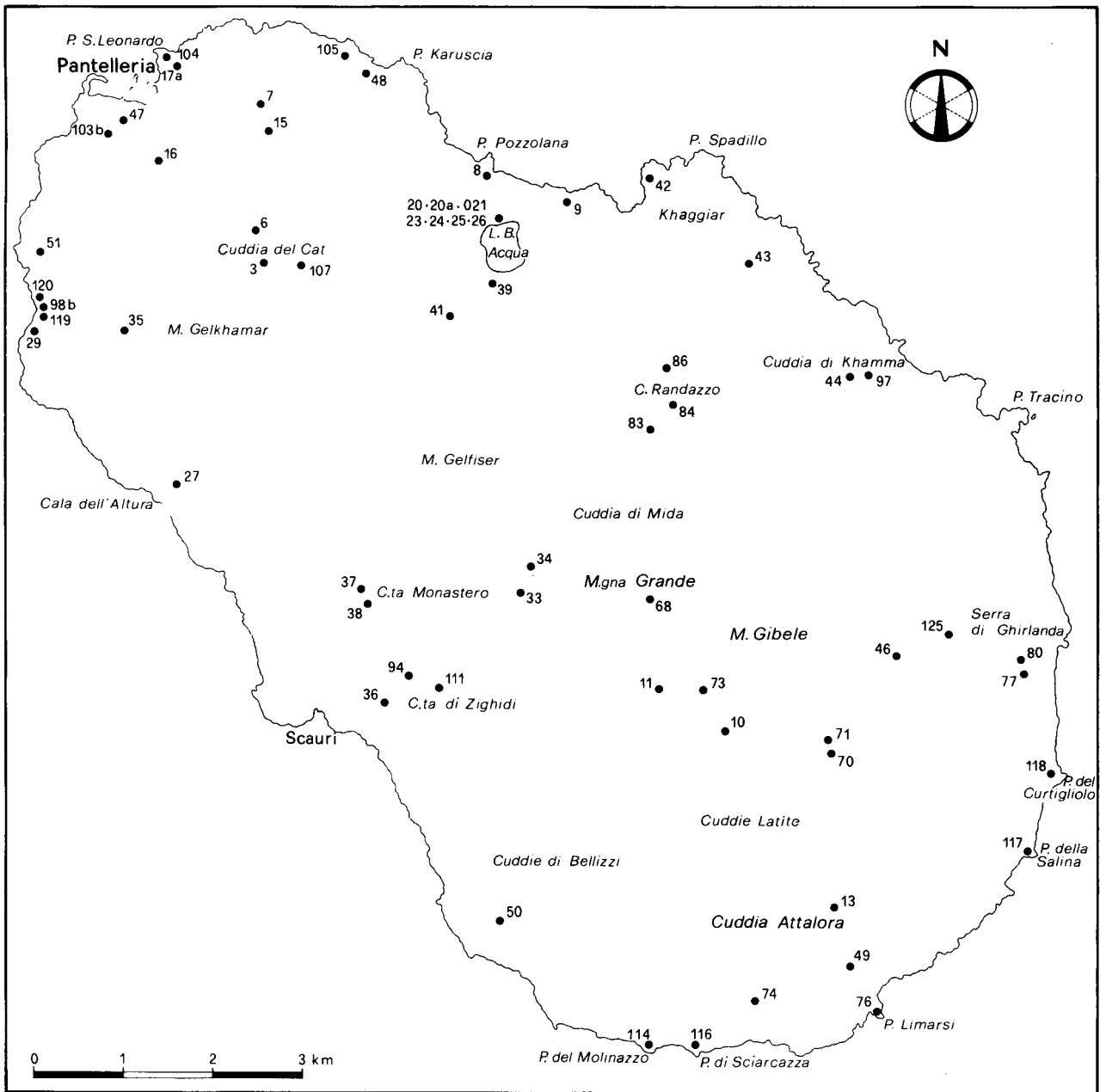


Figure 2. Location map of Pantelleria. Numbers refer to the analysed samples.

hydrated to a high degree ($H_2O^+ \sim 2\%$). Nevertheless significant loss of Na_2O , gain of K_2O or increase of the Fe_2O_3/FeO ratio in respect to chemically comparable dense obsidians have not been detected. Thus it can be reasonably assumed that the measured chemical compositions recalculated free of water and normalized to 100% represent original magma compositions. The major element contents of the analysed rocks of this group define a trend fairly similar to the trend previously described for the green tuff. Moreover Villari (1974b) reports chemical analyses of whole rock, separated glass and anorthoclase phenocrysts of a sample from Montagna Grande dome. The whole rock is slightly metaluminous (similar in composition to samples SIC 73 and SIC 68) while the glass is distinctly peralkaline, shifting towards the composition of the Serra di

Ghirlanda tephra. This stresses the linkage already shown by geometrical relationships and K-Ar dating (Table 1) among the different products of the Montagna Grande volcanic complex. The related magmas can be inferred to have tapped different levels of a compositionally zoned magma chamber. The chemical gap between the pantellerites and the trachytes can either be due to insufficient sampling or represent a genuine compositional gap in the magma chamber.

Basaltic fissure activity (Group D in Table 3) dated at around 29000 a.B.P. (Table 1), occurred contemporaneously with the eruption of the Montagna Grande complex. This activity was localized in the northern part of the island out of both the caldera depressions.

Group E in Table 2 includes two samples from the

Table 4. Neutron activation analyses of silicic and mafic rocks from Pantelleria

Sample no....	10	49	20	35	42	68	53	11	9	3	17a
Eruptive cycle	F	F	B	E	H	C	X	X	C	A	D
Rock type	P	P	P	P	T	T	T	b	h	h	β
SiO ₂ %	70.07	70.01	68.62	68.20	66.35	65.22	64.52	59.60	51.11	47.63	47.96
La (ppm)	296	275	211	213	121	72	77	64	74	49	32
Ce (ppm)	462	431	353	311	218	113	131	107	113	95	53
Nd (ppm)	151	139	136	126	73	42	47	n.m.	n.m.	42	n.m.
Sm (ppm)	37.2	33.3	28.5	23.3	15.5	9.5	10.5	10.1	10.1	9.5	6.7
Eu (ppm)	4.34	4.54	4.36	3.56	3.46	3.56	3.60	3.43	3.70	4.66	2.79
Gd (ppm)	31.8	32.2	26.1	24.4	18.0	11.6	10.5	9.60	9.60	10.5	6.90
Tb (ppm)	6.0	5.9	4.8	4.3	2.9	1.7	1.8	1.5	1.5	1.4	1.0
Yb (ppm)	18	20	17	14	9	6	5	3.5	2.5	2.8	2.0
Lu (ppm)	3.0	2.6	2.2	1.9	1.2	0.73	0.80	0.56	0.40	0.34	0.35
Σ REE	1009.3	943.5	783.0	721.5	426.1	260.1	287.2	255.7	274.8	215.2	140.7
Cs (ppm)	2854	2009	2026	2150	1273	283	297	157	185	199	118
Th (ppm)	43.9	43.4	31.8	33.3	16.3	10.1	11.0	7.7	8.5	4.4	3.0
U (ppm)	13.1	12.7	9.5	9.1	4.7	2.5	3.3	2.0	2.0	1.2	0.67
Hf (ppm)	52.2	50.6	39.6	38.7	19.3	12.5	13.0	9.60	7.02	5.10	3.89
Co (ppm)	0.69	1.49	0.81	1.70	1.37	3.27	3.00	21.3	31.3	42.6	43.6
Sb (ppm)	934	932	710	641	337	230	176	106	95	116	114
Rb (ppm)	189	217	157	165	99	65	69	43	35	22	19
Sr (ppm)	n.d.	n.d.	n.d.	n.d.	n.d.	223	191	333	710	556	466
Ba (ppm)	46	64	80	81	209	1125	1085	859	630	640	321
Sc (ppm)	2.01	1.91	4.08	4.46	5.32	6.44	6.24	19.5	22.3	32.1	33.3
Ta (ppm)	29.1	30.8	22.3	22.7	12.9	8.2	8.7	6.1	4.7	3.4	2.7

n.m. = not measured; n.d. = not detected; p = pantellerite; τ = trachyte; b = benmoreite; h = hawaiite; β = basalt.
All the numbers are preceded by SIC.

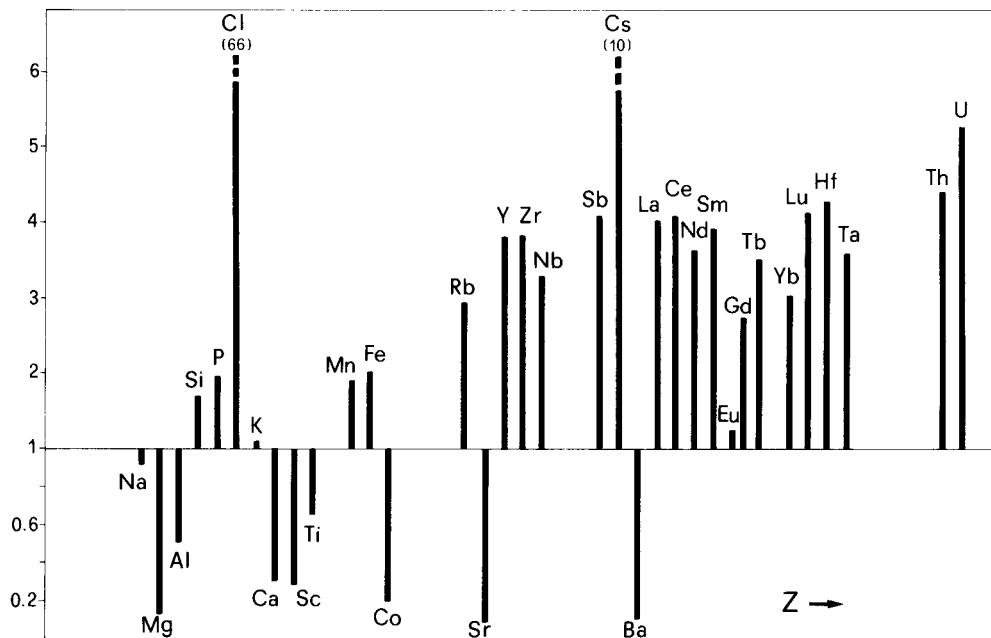


Figure 3. Enrichment and depletion factors of compatible and incompatible elements for a pantellerite (sample SIC 10) relative to a trachyte (sample SIC 68).

Monte Gelkamar dome (Fig. 1; Villari, 1968). Sample SIC 35 was collected from the dome and SIC 29 from a late-stage lava flow. The chemical variations from the first to the latest erupted products define a restricted part of the geochemical trend previously described.

Group F (Lower pantelleritic lava flows and domes) includes samples with different Apatitic index (Table 2), grouped together on the basis of stratigraphic position, morphological evidence and field occurrence although they cannot be arranged in a stratigraphic succession. Therefore the observed geochemical variations are not directly time related.

The volcanic activity younger than the Lower pantelleritic lava flows and domes includes the eruption of: Cuddia di Mida Tephra (Group G in Table 2) dated at 8000 a B.P.; the Khaggiar dome and related lava flows (Group H in Table 2); and Upper pantelleritic lava flows and domes (Group I in Table 2). Radiometric ages for the last two groups are not available as yet. Stratigraphic relationships are known only for the samples of group H, SIC 42 being from the last erupted lava flows. The chemical variations displayed by the analysed rocks of this group define the same trend previously described from pantellerites to trachytes.

Basaltic activity of mildly alkalic composition younger than 10000 a occurred on the northwestern coast of the island (Group L in Table 3). Chemical analyses of xenoliths of trachytic and benmoreitic composition are reported in Tables 2 and 3.

5.b. Trace elements

The silicic rocks are characterized (Tables 2, 3, 4) by a continuous increase of REE, Cs, Rb, Nb, Zr, Y, Ta, Th, U, Sb, Hf and a decrease of Ba, Sr, Co and Sc with increasing differentiation from trachyte to pantellerite. The pattern of enrichment factors is shown in Figure 3. Variation diagrams of selected trace elements (Fig. 4) point to the close coherence of the rocks of all the eruptive silicic cycles.

The main features of the normalized REE patterns (Fig. 5) for increasing SiO_2 content are: (1) increase of total concentration of REE; (2) enrichment in light REE (La to Sm) relative to heavy REE (Gd to Yb); (3) strong development of a negative Eu anomaly ($\text{Eu}/\text{Eu}^* = 1/0.37$); (4) small but progressive enrichment of the heavy REE from Gd to Yb.

The trace element variations observed within and between the various silicic eruptive cycles emphasize the major element variations with time (Table 2). In particular Zr decreases from the first to the last erupted magmas of each cycle and increases again before the beginning of the successive cycle (Fig. 6). All the other analysed elements behave in the same or in the opposite way. Smith (1979) reported a similar pattern (Nb versus time) for the Bandelier Tuff.

Trace element contents of basic and intermediate rocks are reported in Tables 3 and 4. Chondrite-normalized rare earth patterns are reported in Figure 5. The abundance of transition metals (Sc, V, Cr, Co, Ni) decreases with increasing SiO_2 . Large ion lithophile element contents increase with SiO_2 , ranging from 45.5 to 57.2% except Sr which reaches its highest

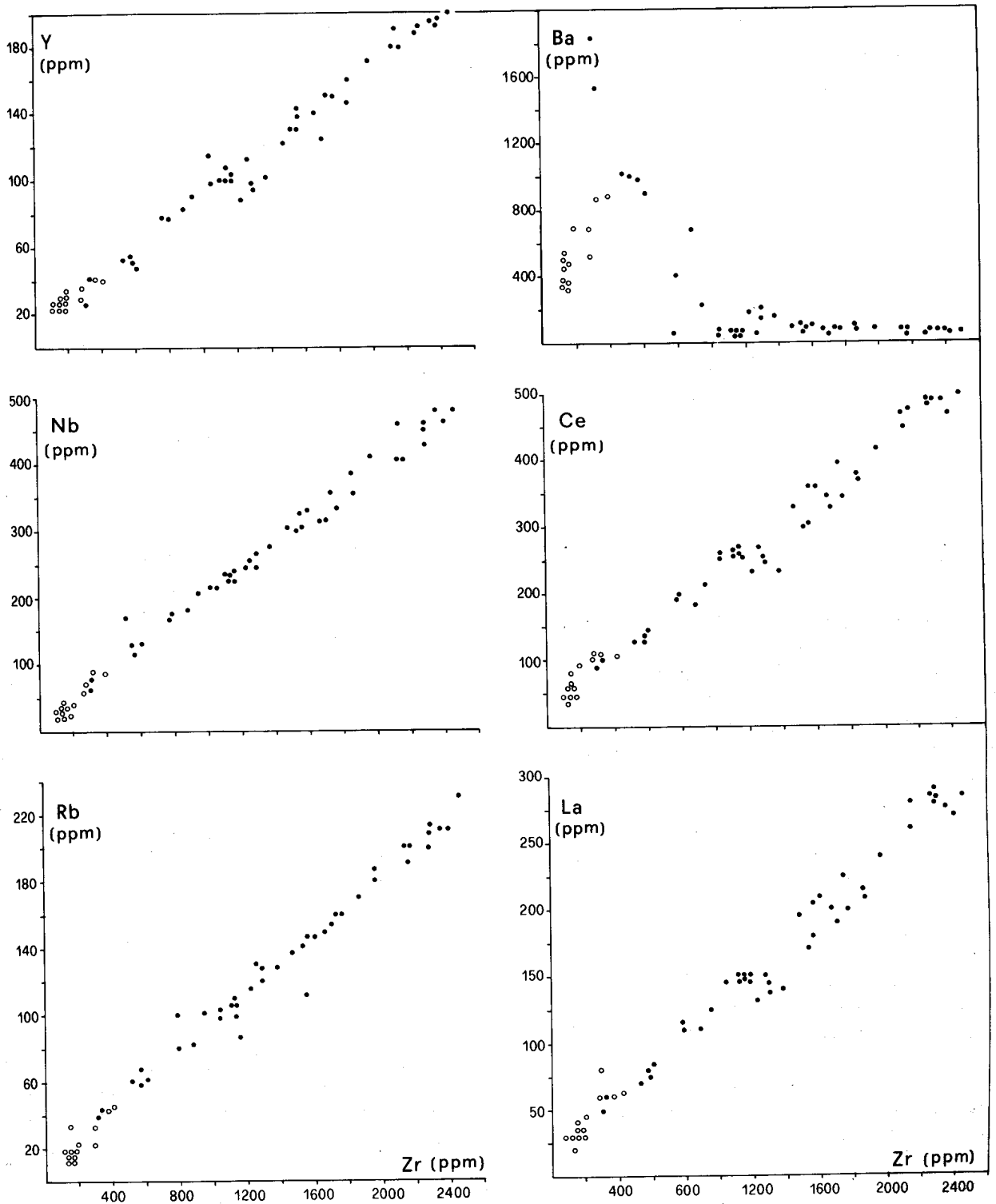


Figure 4. Variation of selected trace elements with Zr. ●, Silicic rocks; ○, mafic and intermediate rocks.

concentration for SiO_2 value of 51.1%. All the analysed samples are fractionated for both light and heavy REE (Fig. 5). Basalts, hawaiites and benmoreites have similar REE abundance patterns despite variation in absolute abundance. Samples SIC 17 and SIC 3 have a significant positive Eu anomaly. Plagioclase is the most abundant phenocryst

in these rocks and the anomaly could be explained by relative accumulation of plagioclase during magma ascent.

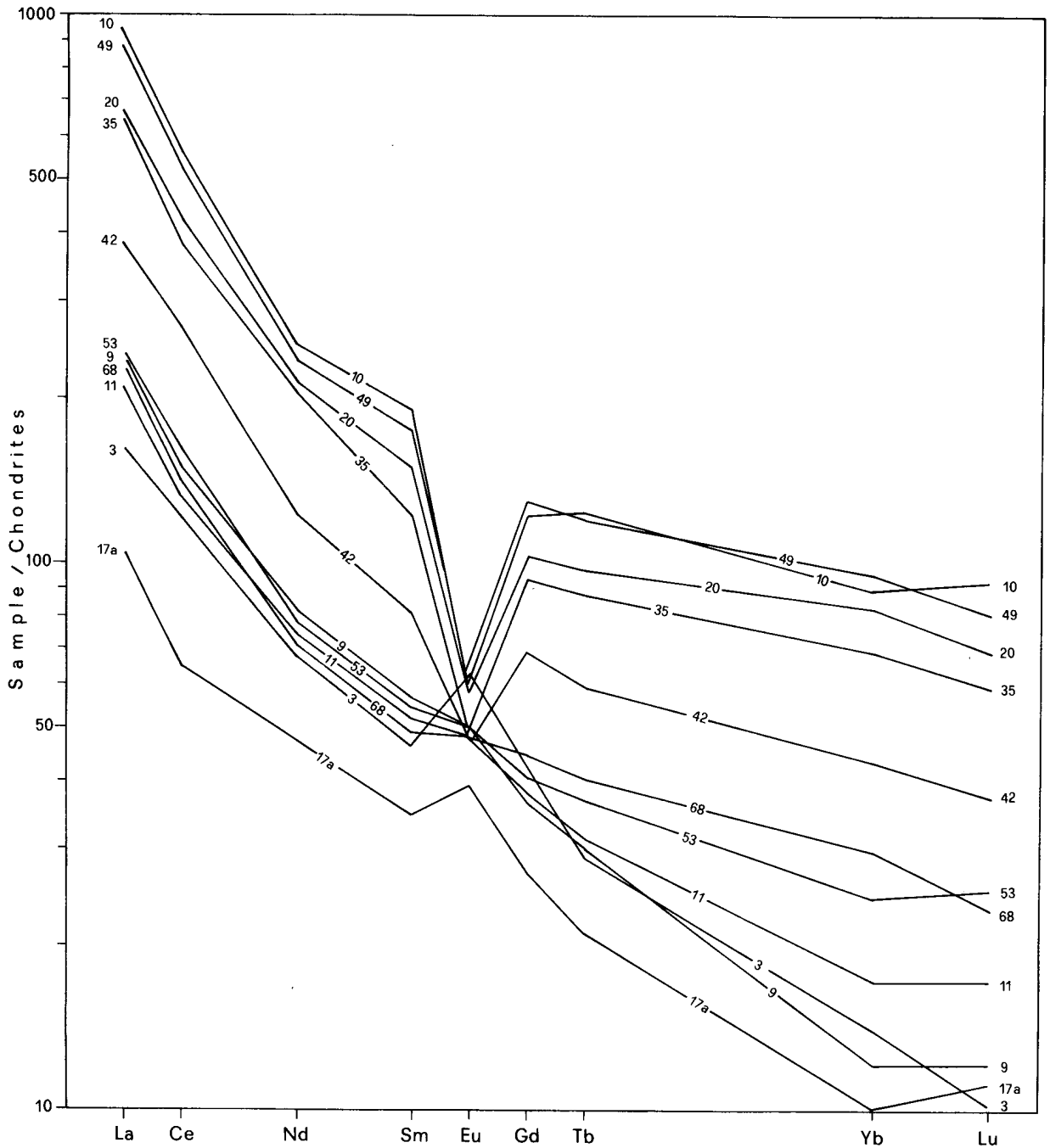


Figure 5. Rare earth pattern normalized to chondrites; normalizing values are the Leedley chondrite data (Masuda, Nakamura & Tanaki, 1973), divided by 1.20. Sample nos. 49, 10, 20 and 35 = pantellerites; sample nos. 42, 53 and 68 = trachytes; sample no. 11 = benmoreite; sample no. 9 = mugearite; sample no. 3 = hawaiiite; sample no. 17a = mildly alkalic basalt.

5.c. Sr-isotope ratios

$^{87}\text{Sr}/^{86}\text{Sr}$ ratios of the five analysed basaltic rocks range from 0.70280 ± 6 to 0.70297 ± 4 (Table 5). Two trachytes and one benmoreitic xenolith give Sr-isotopic ratios of 0.70306 ± 1 (mean of two analyses), and 0.70310 ± 4 respectively. These values are similar within the analytical error to those measured for the radiogenic basalts.

Initial $^{87}\text{Sr}/^{86}\text{Sr}$ ratios of the pantellerites range from $0.70335 (\pm 4)$ to $0.70852 (\pm 8)$. For one sample (SIC 20; Table 5) Sr-isotope ratios have been measured on

whole rock and on a feldspar separate. The results agree within analytical error. Korrington & Noble (1972) report Sr-isotope compositions of 0.070304 ± 15 and 0.70291 ± 15 for a trachyte and of 0.70305 ± 20 for a pantellerite. The large Sr-isotope variation displayed by the pantellerites is not related either to the Sr concentrations (Fig. 7) or to any other chemical parameter. Furthermore no correlations among $^{87}\text{Sr}/^{86}\text{Sr}$ ratios, time of eruption and stratigraphic position of each sample have been identified. This wide range of Sr-isotopic composition for pantellerites is apparently inconsistent with the close genetic relation

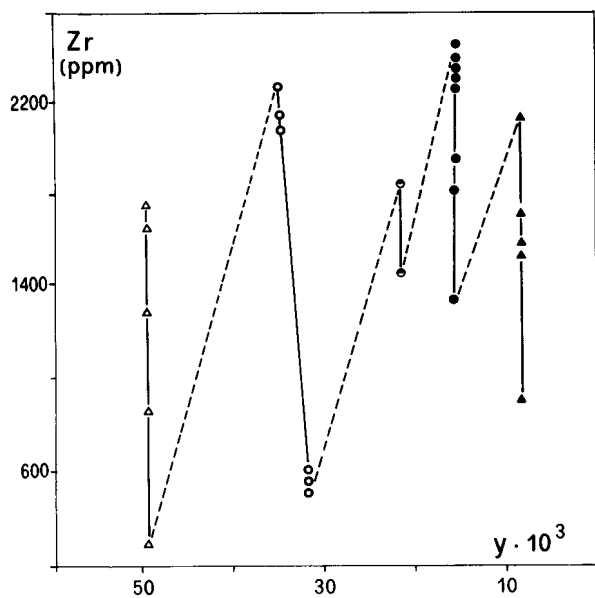


Figure 6. Zr variation with time. Δ , Green tuff; \circ , Montagna Grande volcanic complex; \bullet , Gelkhamar dome; \bullet , Lower pantelleritic lava flows and domes; \blacktriangle , Cuddia di Mida tephra and Khaggiar dome.

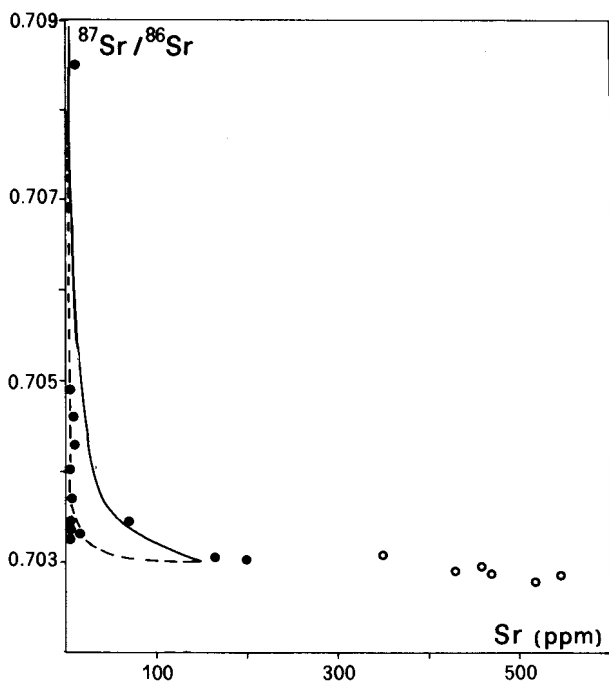


Figure 7. $^{87}\text{Sr}/^{86}\text{Sr}$ of mafic and silicic rocks plotted against Sr content. \bullet , Silicic rocks; \circ , mafic and intermediate rocks. Lines correspond to fractional crystallization combined with crustal assimilation modelling considering an assimilation/crystallization velocity ratio of 0.1 and a bulk partition coefficient of 5. Dotted and continuous lines correspond to contaminant compositions of 100 ppm of Sr and 0.720 Sr-isotope ratio and of 20 ppm of Sr and 0.709 Sr-isotope ratio respectively.

Table 5. Sr-isotope composition of mafic and silicic rocks from Pantelleria

Sample no.	Rock* type	Eruptive† cycle	Age (10 ³ a)	Rb/Sr‡	$^{87}\text{Sr}/^{86}\text{Sr}$ measured	$^{87}\text{Sr}/^{86}\text{Sr}$ initial
SIC 3	β	A	120000	0.041	0.70287 \pm 4	0.70287 \pm 4
SIC 16	β	D	29000	0.035	0.70280 \pm 6	0.70280 \pm 6
SIC 48	β	D	29000	0.037	0.70297 \pm 4	0.70297 \pm 4
SIC 17a	β	D	29000	0.036	0.70289 \pm 5	0.70289 \pm 5
SIC 51	β	L	< 10000	0.033	0.70292 \pm 6	0.70292 \pm 6
SIC 44	P	A	> 50000	12.3	0.70431 \pm 6	0.70429 \pm 6§
SIC 27	P	A	> 50000	9.4	0.70854 \pm 8	0.70852 \pm 8§
SIC 23	τ	A	> 50000	1.20	0.70345 \pm 4	0.70345 \pm 4§
SIC 20	P	B	50000	106	0.70359 \pm 7	0.70338 \pm 7
SIC 20a	P	B	50000		0.70357 \pm 4	
SIC 33	τ	C	35000	0.68	0.70307 \pm 5	0.70307 \pm 5
SIC 68	τ	C	35000	0.29	0.70305 \pm 5	0.70305 \pm 5
SIC 35	P	E	22000	44.2	0.70494 \pm 6	0.70490 \pm 6
SIC 43	P	F	16000	38.9	0.70333 \pm 6	0.70330 \pm 6
SIC 49	P	F	16000	76.7	0.70340 \pm 4	0.70335 \pm 4
SIC 50	P	F	16000	16.7	0.70461 \pm 16	0.70460 \pm 16
SIC 41	P	F	16000	48.6	0.70371 \pm 5	0.70368 \pm 5
SIC 10	P	F	16000	50.5	0.70335 \pm 6	0.70332 \pm 6
SIC 34	P	G	9000	94.8	0.70406 \pm 6	0.70403 \pm 6
SIC 11	B			0.13	0.70309 \pm 5	0.70309 \pm 5

* β = basalt; P = pantellerite; τ = trachyte; B = benmoreite.

† = eruptive cycle letters are defined in the text and in Tables 2 and 3.

‡ = Rb and Sr concentrations measured by X-ray fluorescence, see Tables 2 and 3.

§ = $^{87}\text{Sr}/^{86}\text{Sr}$ initial values calculated using an age of 50000 a.

All the Sr-isotope compositions have been measured on whole rock samples except SIC 20 for which a feldspar separate was analysed (SIC 20a).

between the trachytes and pantellerites indicated by field occurrence and systematic chemical variations. Different $^{87}\text{Sr}/^{86}\text{Sr}$ values in suites of apparently comagmatic rocks are a feature of other peralkaline associations (Dickinson, Dodson & Gass, 1969; Dickinson & Gibson, 1972).

6. Discussion

The most interesting problems arising from the data are: (1) the origin of the compositional trends displayed either by the products of each eruptive cycle or by the silicic rocks as a whole and (2) the genetic relationships, if any, between mafic and silicic rocks.

6.a. Origin of the compositional trends

The chemical variations repeatedly displayed by the Pantelleria silicic rocks over the last 220000 years are probably the result of similar differentiation processes. These processes have generated an increase of SiO_2 , REE, Rb, Zr, Nb, Y, Ta, Hf, Cl, Th, U and a decrease of Al_2O_3 , CaO, MgO, Sr, Ba in the high levels of the magma chamber. The most popular mechanisms proposed to explain the compositional variations of the silicic rocks are: (a) incremental partial melting of a common source; (b) fractional crystallization of a parental magma of trachytic composition; (c) thermogravitational diffusion (Shaw, Smith & Hildreth, 1976; Hildreth, 1979; Smith, 1979).

6.a.1. Incremental partial melting

Progressive partial melting of a source region and incremental accretion to a growing magma reservoir cannot produce the geochemical variations observed for the silicic rocks of Pantelleria. The most critical evidences against this model are the very low concentrations of Ba and Sr in many pantellerites and the very steep gradients of these elements from pantellerites to trachytes. Simple partial melting model calculations starting from a feldspar-rich source material characterized by bulk coefficients (D) for Ba and Sr greater than 1, show the impossibility of producing large variations in the concentrations of these elements as the range is limited by $1/D$ (Shaw, 1970; Hanson, 1978).

6.a.2 Fractional crystallization

A least squares mixing model (Stormer & Nicholls, 1978) was used to test a mechanism involving fractionation of a trachytic magma to produce a pantelleritic liquid (Table 6). The model shows that crystal fractionation of anorthoclase, aenigmatite, ferrohedenbergite and fayalite can account for the chemical variations displayed either by each eruptive cycle or by the silicic rocks as a whole. The compositional range displayed

Table 6. Results of least squares calculation of major element concentrations of silicic rocks from different eruptive cycles of Pantelleria

From initial composition to final composition	Eruptive cycle	Solid phases to be removed (wt %)					F	R ²
		Fayalite (01-1B)	Ferrohedenbergite (Cpx-1)	Anorthoclase (Fid-2)	Anorthoclase (Pan-5S)	Aenigmatite (Cos-3A)		
From SIC 94 to SIC 97	B	2.25	1.40	43.85	45.07	7.43	75.58	0.12
From SIC 94 to SIC 76	B	7.96	0.94	31.68	59.42	—	52.77	0.30
From SIC 76 to SIC 97	B	4.04	1.86	59.57	30.87	3.66	49.93	0.09
From SIC 68 to SIC 125	C	2.35	1.92	18.09	75.42	2.21	77.30	0.48
From SIC 50 to SIC 37	F	0.19	5.41	88.83	3.38	2.19	43.78	0.29
From SIC 84 to SIC 34	G	13.07	0.0	48.90	35.27	2.76	13.60	0.13
From SIC 42 to SIC 86	H	1.97	13.47	79.63	0.0	4.93	42.42	0.10
From SIC 68 to SIC 10	—	3.61	2.00	25.64	68.16	0.59	77.45	0.80

Eruptive cycle letters are defined in the text and in Table 2.

Chemical analyses of 01-1B, Cpx-1, Fid-2, Cos-3A are Carmichael (1962) and of Pan-5S from Villari (1974b). Fid-2 and Pan-5S have different chemical compositions. F = total wt % of solid fractionated. R² = is the sum of the residues squared. SIC 68 and SIC 10 belong to different eruptive cycles.

Table 7. Results of least squares calculation of trace element concentrations of silicic rocks from different eruptive cycles of Pantelleria

From initial composition to final composition	Eruptive cycle	F	F ₁	R ²
From SIC 94 to SIC 97	B	75.58	79.62	0.04
From SIC 68 to SIC 125	C	77.30	75.41	0.02
From SIC 33 to SIC 125	C	91.34	80.91	0.06
From SIC 50 to SIC 37	F	43.78	47.04	0.14
From SIC 84 to SIC 34	G	13.60	24.74	0.06
From SIC 42 to SIC 86	H	42.42	47.27	0.27
From SIC 68 to SIC 10	—	77.45	77.57	0.01

F is as defined in Table 6 and is reported for comparison with F₁. F₁ = total wt (%) of solid fractionated calculated using the Rayleigh fractionation equation.

Fractionating minerals are those in Table 6. Distribution coefficients are from Arth (1976), Willemant *et al.* (1981), Pearce & Norry (1979), Mahood (1981), Korrington & Noble (1971) and Drexler, Burnhorst & Noble (1983).

R² = is the sum of the residues squared; the residues are the differences between the F₁ calculated for each element and the mean value of F₁.

SIC 68 and SIC 10 belong to different eruptive cycles.

by the green tuff has been further broken down into smaller portions for modelling. The results show that, in agreement with mineralogical evidence, aenigmatite

represents a late-crystallizing phase (Table 6). Although these solutions are not unique, they suggest that fractional crystallization could have occurred as a repetitive process in the Pantelleria system.

Trace element modelling (Table 7) supports the results of the major element calculations. The fraction of solid removed (F) can be calculated by the Rayleigh equation using the mineral proportions generated by major element modelling. The main assumption made for the trace element modelling concerns the selection of distribution coefficients (D.C.) from the literature. This can be misleading considering the variations of D.C. with melt compositions, temperatures and other intensive parameters, including volatile component activities (Hildreth & Mahood, 1982). The agreement between the F values of both major and trace elements modelling is good. Figure 8 compares the observed and calculated trace element pattern of a pantellerite normalized with respect to a trachyte. The results of major and trace element modelling suggest that the pantellerites represent 20 to 40% fractional crystallization of trachytic parent liquids. The greatest degree of fractionation is required for the pantellerites of Serra di Ghirlanda and for the Lower pantelleritic lava flows and domes.

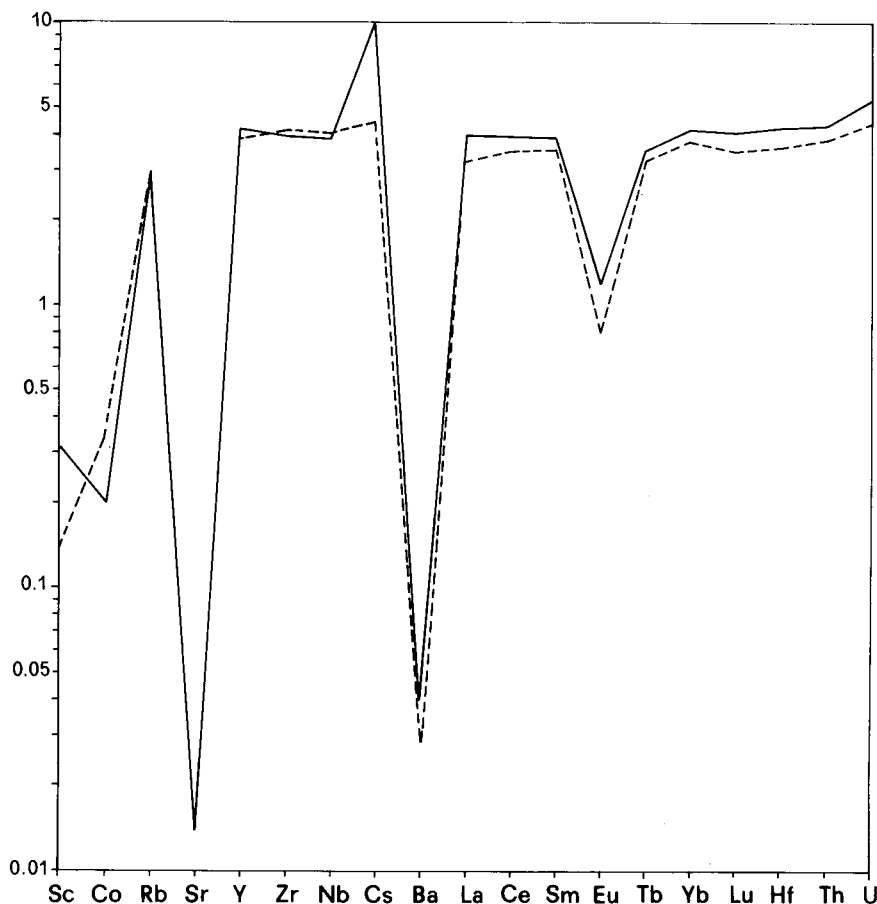


Figure 8. Diagram comparing the trace element pattern of measured (—) and predicted (---) daughter magma normalized to the presumed parent. The daughter and parent magmas are assumed to be represented by samples SIC 10 and SIC 68 respectively.

6.a.3. Convection-driven thermogravitational diffusion

This process involves the combined effects of convective circulation and Soret diffusion to develop chemical gradients within the thermal and gravitational fields existing in magma chambers (Shaw, Smith & Hildreth, 1976; Hildreth, 1977, 1979, 1981; Smith, 1979). The peralkaline magmatic system of Pantelleria exhibits a chemical zonation with Zr, Hf, LREE strongly concentrated roofward together with all the other trivalent REE, Th, U, Ta, Cs, Rb, Y, Nb, Cl. Hildreth (1981) attributes this pattern to thermogravitational and volatile complexing processes, the enrichment in Nb, Zr, Hf, REE being closely linked to roofward migration of Cl.

Differentiation mechanisms involving the Soret diffusion or volatile transport cannot be quantitatively modelled as yet. We cannot exclude that such processes have operated in the magmatic system of Pantelleria. If that is the case their effects simulate those expected by crystal fractionation, as shown above. Therefore we would rather accept a fractional crystallization process which can quantitatively account for the major- and trace-element variations displayed by the products of each eruptive cycle. Two main objections can be made against this process. The first is based on the physical properties of silicic magmas (see Sparks *et al.* 1984, for a review). Considering the high viscosity of rhyolitic magmas it is doubtful that the minerals of different densities would separate from the melt in the proportion suggested by major- and trace-element modelling. Furthermore phenocrysts are generally unzoned. Fractionation could have taken place by accretion of crystals on the walls of the magma chamber with consequent migration of a rhyolitic boundary layer to the upper part of the chamber (McBirney, 1980) or by convective separation of residual liquid from growing crystals (Sparks *et al.* 1984). The second objection arises from the higher and more scattered $^{87}\text{Sr}/^{86}\text{Sr}$ ratios of the pantellerites with respect to the trachytes (Table 5).

The pantellerites characterized by very low Sr concentration, are very susceptible to contamination either by foreign groundwater-transported Sr, which on Pantelleria contains appreciable Sr of sea water origin, or by crustal material during the storage of their magma in the magma chamber. The similar Sr-isotope composition measured for a pantelleritic whole rock sample and anortoclase separate (Table 5) suggests that contamination took place within the magma chamber. Figure 7 illustrates the combined effect of fractional crystallization and contamination (AFC, De Paolo, 1981) on an initial trachytic magma characterized by a Sr concentration of 150 ppm and with a $^{87}\text{Sr}/^{86}\text{Sr}$ of 0.70305. The value adopted for r (ratio between velocities of assimilation and crystallization) is 0.1. The Sr bulk distribution coefficient used is 5, in agreement with the results of trace-

element modelling. Two contaminating materials with Sr concentrations of 100 and 20 ppm and Sr-isotope ratios of 0.720 and 0.709 respectively have been used for the calculation as presumably representative of upper crustal igneous rocks and marine sediments. The results indicate that the wide range of Sr-isotope compositions displayed by the pantellerites can be accommodated by a combined process of fractional crystallization and contamination with upper crustal igneous rocks and/or marine sediments.

6.b. Genetic relationships between mafic and silicic rocks

The available stratigraphic, petrographic and chemical data (this paper; Cornette *et al.* 1983; Villari, 1974*b*; Korrington & Noble, 1972) suggests that the pantellerites are differentiated, via crystal-liquid fractionation of a trachytic magma. What then is the origin of the trachytic magma? Is it a primary magma or one batch sampled from a much longer line of descent? The $^{87}\text{Sr}/^{86}\text{Sr}$ ratios reported here in for the trachytes (Table 5) range from 0.70305 ± 4 to 0.70307 ± 4 . These values are similar within the errors to the $^{87}\text{Sr}/^{86}\text{Sr}$ ratio of the basalt most enriched in radiogenic Sr (0.70297 ± 4) suggesting a genetic relation between basalts and trachytes.

Therefore the viable mechanisms for the generation of the peralkaline trachytic magmas of Pantelleria remain: (a) fractional crystallization of a mafic parental magma; (b) partial melting of a mafic source. These two mechanisms essentially involve an ultimate mantle derivation for the trachytic magmas. In the second case, the mafic magma solidifies near the base of the crust before partially melting to produce the trachytic liquid.

6.b.1. Fractional crystallization of a mafic magma

Derivation of the trachytes from a mafic parental magma by fractional crystallization explains the salient chemical features of the trachytic rocks, namely their depletion in Ni, Co, Sr, Sc and P and their enrichment in most incompatible elements. Sr, P, Ni, and Co may have been extracted by the observed phenocrysts: plagioclase, apatite, olivine and pyroxene. The enrichment in most of the incompatible elements is explained by their concentration in the liquid phase during crystal fractionation. This hypothesis was tested using the least-squares major-element mixing calculation (Stormer & Nicholls, 1978) and trace-element modelling previously described. The results of these calculations show that the transition from basalts to trachytes (from SIC 17 to SIC 68) can be explained by fractional crystallization of 81.7% of a solid containing 55.8% of plagioclase, 29.5% of clinopyroxene, 3.3% of olivine, 2.6% of apatite and 8.8% of magnetite. Sample SIC 17 was chosen as the parent because it is one of the less differentiated analysed lavas. Such a model can be

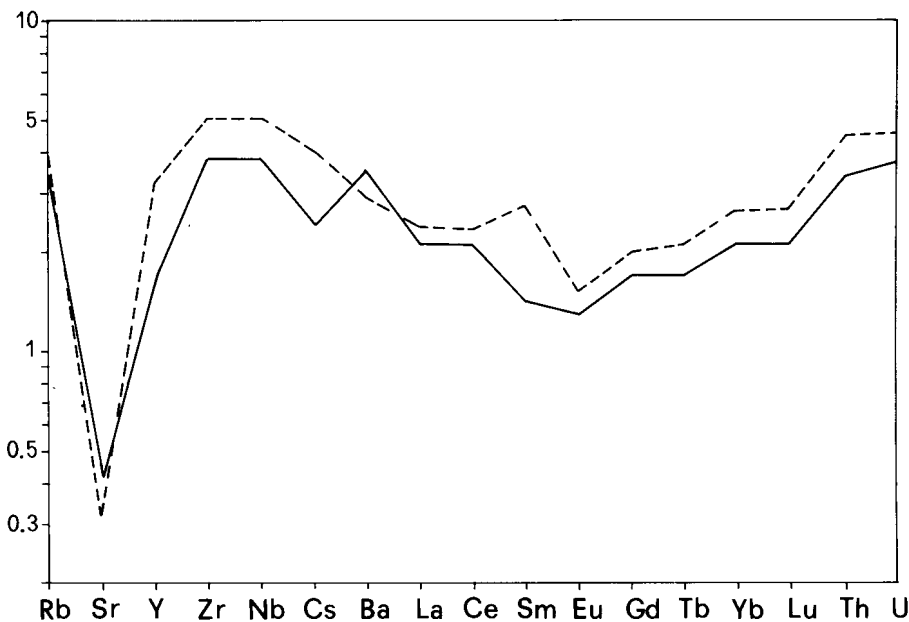


Figure 9. Diagram comparing the trace element pattern of measured (—) and predicted (---) daughter magma normalized to the presumed parent melt. The daughter and parent magmas are assumed to be represented by samples SIC 68 and SIC 17a respectively.

further verified by trace element calculation using the Rayleigh fractionation equation. Mineral proportions used in this calculation were taken from the major-element modelling. The solutions are reported in Figure 9 and are in agreement with the results of major-element modelling although they require a slightly greater degree of fractionation. The already mentioned similarity between the Sr isotopic compositions of basalts and trachytes supports this model. Furthermore the benmoreite xenoliths previously described can represent a genetic link between mafic and silicic peralkaline rocks. A gravimetric study (Gantar *et al.* 1961; Berrino *et al.* 1984) has shown the existence of a large body of high density material ($\rho = 0.003 \text{ kg/m}^3$) at shallow depth beneath the island of Pantelleria. This could represent the residual of the mafic parental magma required by fractional crystallization.

6.b.2. Partial melting of a mafic source

Remelting of a mafic magma body generated by large scale partial fusion in the mantle and crystallized at deep crustal levels could account for the generation of the trachytic magmas. This model conveniently explains the volume relations and the existence of a compositional gap between silicic and mafic rocks. The mineralogy of the mafic magma crystallized at deep crustal levels is likely to be olivine + clinopyroxene + plagioclase. The trace-element pattern of a liquid generated from equilibrium partial melting of a source with the above mineralogy and with composition similar to that of the less evolved basaltic rocks of Pantelleria could reproduce the pattern of the trachytes.

Quantitative modelling of such a process is not attempted owing to the many unknown parameters which should be considered in the calculation.

7. Conclusions

Major- and trace-element and Sr-isotope data are consistent with the following hypothesis on the origin of the silicic rocks from Pantelleria. Trachytic parent magma with initial $^{87}\text{Sr}/^{86}\text{Sr}$ ratio of about 0.703 was generated either by fractional crystallization from more mafic mantle-derived magma or by melting of a young gabbroic intrusion. We prefer the first hypothesis as it better accounts for the geochemical, isotopic and gravimetric data. The trachytic parent magma differentiated in a low pressure magma chamber by crystal-liquid fractionation. This process resulted in a compositionally zoned magma chamber. During low pressure crystal-liquid differentiation the $^{87}\text{Sr}/^{86}\text{Sr}$ ratio of some of the most evolved Sr-poor rhyolitic magmas increased up to a value of 0.708 by contamination with crustal material.

Constraints on the physical properties of the magma chamber derive from the occurrence of silicic and mafic eruptive cycles separated by short repose time with the basaltic activity localized outside the caldera depressions, at least in the last 50000 years. This implies that basaltic magmas were apparently unable to reach the surface in the area of the caldera depression probably because of the presence of a magma body within the crust. The wide compositional range displayed by the products of each silicic eruptive cycle testifies that the previously mentioned differentiation processes operated several times in the magma chamber. Furthermore

inspection of Figure 6 shows that the degree of chemical evolution of the rhyolites of the different cycles did not vary in time in a simple progressive way but that a rather similar range of chemical variations is displayed in many of the eruptive cycles. This evidence supports an open system behaviour of the magma chamber which is probably episodically refilled by more mafic (trachytic or basaltic) parent magma, differentiated at high rate and episodically erupted. High rates of differentiation are suggested by the short repose time between compositionally zoned eruptions (Fig. 6), the varied range of composition erupted during each eruptive cycle and the small erupted volumes (always less than 2 km³; Orsi, unpublished data). This implies the existence of a small magma chamber which stratifies or becomes chemically zoned at a higher rate than systems with large volumes (Spera & Crisp, 1981).

8. Addendum

After this article was submitted for publication G. Mahood and W. Hildreth published a paper entitled 'Nested calderas and trapdoor uplift at Pantelleria, Strait of Sicily' (*Geology* **11**, 722–6, 1983), in which they present a reconstruction of the geological history of Pantelleria greatly differing from the first proposed by the same authors (Mahood & Hildreth, 1980). Their model is for many aspects in agreement with the one previously published by Cornette *et al.* (1982, 1983) and detailed in this paper. The main differences concern the structural setting of the island and the definition and evolution of the Montagna Grande Volcanic complex as defined by Cornette *et al.* (1982, 1983). They do not recognize the pantelleritic Serra di Ghirlanda tephra as part of this eruptive cycle. Therefore, according to them, all the products of this cycle are trachytic in composition and should represent the deeper level of a stratified magma chamber. Also the ages they define for this cycle differ from ours. They report a range from 49000 to 33000 a B.P. but for both these and the other ages presented they do not give any indication on location of the dated samples. Consequently comparison with our results is impossible.

Acknowledgements. This work was financially supported by the Italian M.P.I. and by the National Council of Scientific Research of France; Programme interdisciplinaires des Recherches pour la prévision et la surveillance des éruptions volcaniques. The Sr-isotope work was carried out while one of the authors (Lucia Civetta) was at the Department of Earth Sciences, University of Leeds, England; Lucia Civetta gratefully acknowledges the friendly help given by all the staff of the Isotopic Group. The authors thank Dr Sparks for critical reading of the manuscript and useful suggestions.

References

- AGOCs, W. B. 1959. Profondità e struttura dell'orizzonte igneo tra Catania e Tunisi dedotta da un profilo aeromagnetico. *Bollettino del Servizio Geologico Italiano* **80**, 51–61.
- ARTH, J. G. 1976. Behavior of trace elements during magmatic processes. Summary of theoretical models and their applications. *Journal of Research of U.S. Geological Survey* **4**, 41–7.
- BACON, C. R., MACDONALD, R., SMITH, R. L. & BAEDECKER, P. A. 1981. Pleistocene high-silica rhyolites of the Coso volcanic field, Inyo County, California. *Journal of Geophysical Research* **86**, 10223–41.
- BAILEY, D. K. & MACDONALD, R. 1975. Fluorine and chlorine in peralkaline liquids and the need for magma generation in an open system. *Mineralogical Magazine* **40**, 405–14.
- BERRINO, G., CASTELLANO, M., DEL GAUDIO, G., D'ERRICO, V., FRANCHINO, A., GRIMALDI, M. & RICCO, C. 1984. Anomalie gravimetriche e noise sismico a Pantelleria. *Bollettino della Società dei Naturalisti* (in press).
- BIGAZZI, G., BONADONNA, F. P., BELLUOMINI, G. & MALPIERI, L. 1971. Studi sulle ossidiane italiane. IV. Datazione con il metodo delle tracce di fissione. *Bollettino della società Geologica Italiana* **90**, 469–80.
- BIGAZZI, G., BONADONNA, F. P. & RADI, G. 1982. Fission track dating of obsidians and prehistory. Collection of the abstracts of the Fission Track method workshop. Fifth International Conference on Geochronology, Cosmochronology and Isotope Geology. Nikko, Japan.
- BORSI, S., MARINELLI, G., MAZZONCINI, F., MITTEMPERGER, U., & TEDESCO, C. 1963. Reconnaissance of some ignimbrites of Pantelleria and Eolian Islands. *Bulletin Volcanologique* **25**, 359–67.
- BRYAN, W. B. 1970. Alkaline and peralkaline rocks of Socorro Island, Mexico. *Carnegie Institution of Washington, Yearbook* **68**, 194–200.
- CARMICHAEL, I. S. E. 1962. Pantelleritic liquids and their phenocrysts. *Mineralogical Magazine* **33**, 86–113.
- CARMICHAEL, I. S. E. 1967. The iron–titanium oxides of salic volcanic rocks and their associated ferromagnesian silicates. *Contributions to Mineralogy and Petrology* **14**, 36–64.
- CASSIGNOL, C., CORNETTE, Y., DAVID, B. & GILLOT, P. Y. 1978. Technologie potassium–argon. Rapport CEA-R 4908, Centre d'Etudes Nucléaires, Saclay, 1–35.
- CASSIGNOL, C. & GILLOT, P. Y. 1982. Range and effectiveness of unspiked potassium–argon dating. In *Numerical Dating in Stratigraphy* (ed. G. Odin), pp. 159–79. New York: Wiley.
- CASSINIS, R., FRANCIOSI, R., & SCARASCIA, S. 1979. The structure of the earth's crust in Italy. A preliminary typology based on seismic data. *Bollettino di Geofisica Teorica ed Applicata* **XXI–81**, 105–25.
- CHAYES, F. & ZIES, E. G. 1962. Sanidine phenocrysts in some peralkaline-volcanic rocks. *Carnegie Institution of Washington, Yearbook* **61**, 112–18.
- CHAYES, F. & ZIES, E. G. 1964. Notes on some Mediterranean comendite and pantellerite specimens. *Carnegie Institute of Washington, Yearbook* **63**, 186–93.
- COLANTUONI, P. & ZARUDZSKI, E. F. K. 1973. Some principal sea floor features in the Strait of Sicily. *Rapport. Congrès International de la Mer Méditerranée* **22** (2a), 68–70.
- COLOMBI, B., GIESE, P., LUONGO, G., MORELLI, C., RIUSCETTI, M., SCARASCIA, S., SCHUTTE, K. G., STROWALD, J. & DE

- VISENTINI, G. 1973. Preliminary report on the seismic refraction profile Gargano-Salerno-Palermo-Pantelleria (1971). *Bollettino di Geofisica Teorica ed Applicata* XV-59, 225-54.
- CORNETTE, Y., CRISCI, G. M., GILLOT, P. Y. & ORSI, G. 1982. The recent volcanic history of Pantelleria: a new interpretation based on geological and geochronological data. In *Workshop on Explosive Volcanism, Program and abstracts*. Italy, May 1982.
- CORNETTE, Y., CRISCI, G. M., GILLOT, P. Y. & ORSI, G. 1983. Recent volcanic history of Pantelleria: a new interpretation. In *Explosive Volcanism* (ed. M. F. Sharidan & F. Barbieri). *Journal of Volcanology and Geothermal Research* 17, 361-73.
- DE PAOLO, D. J. 1981. Trace element and isotopic effects of combined wallrock assimilation and fractional crystallization. *Earth and Planetary Science Letters* 53, 189-202.
- DICKINSON, D. R., DODSON, M. R. & GASS, I. G. 1969. Correlation of initial $^{87}\text{Sr}/^{86}\text{Sr}$ with Rb/Sr in some late Tertiary volcanic rocks of south Arabia. *Earth and Planetary Science Letters* 6, 84-90.
- DICKINSON, D. R. & GIBSON, I. L. 1972. Feldspar fractionation and anomalous $^{87}\text{Sr}/^{86}\text{Sr}$ ratios in a suite of peralkaline silicic rocks. *Geological Society of America Bulletin* 83, 231-40.
- DREXLER, J. W., BORNHORST, T. J. & NOBLE, D. C. 1983. Trace element sanidine/glass distribution coefficients for peralkaline silicic rocks and their implications to peralkaline petrogenesis. *Lithos* 16, 265-71.
- FLYNN, R. T. & BURNHAM, C. W. 1978. An experimental determination of rare earth partition coefficients between a chloride containing vapor phase and silicate melts. *Geochimica et Cosmochimica Acta* 42, 685-701.
- FOERSTNER, H. 1881. Nota preliminare sulla geologia dell'isola di Pantelleria secondo gli studi fatti negli anni 1874 e 1881. *Bollettino del Reale Comitato Geologico d'Italia* 12, 523-56.
- FRANZINI, M. & LEONI, B. 1972. A full matrix correction in X-ray fluorescence analysis. *Atti della Società Toscana di Scienze Naturali* 79, 7-22.
- GANTAR, C., MORELLI, C., SEGRE, A. G. & ZAMPIERI, L. 1961. Studio gravimetrico e considerazioni geologiche sull'isola di Pantelleria. *Bollettino di Geofisica Teorica ed Applicata* III-12, 267-87.
- GILLOT, P. Y. 1978. K-Ar dating of the Laschamp magnetic excursion: a method for young volcanic rock dating. *U.S. Geological Survey Open File Report* 78-701, 140-2.
- GILLOT, P. Y., CHIESA, S., PASQUARE, G. & VEZZOLI, L. 1982. 33,000 yr K-Ar dating of the volcano-tectonic horst of the island of Ischia, Gulf of Naples. *Nature* 299 (5880), 242-4.
- GILLOT, P. Y., LABEYRIE, J., LAJE, C., VALLADAS, G., GUERIN, G., POUPEAU, G. & DELIBRIAS, G. 1979. Age of the Laschamp magnetic excursion revisited. *Earth and Planetary Science Letters* 42, 444-50.
- GILLOT, P. Y. & NATIVEL, P. 1982. K-Ar chronology of the ultimate activity of Piton des Neiges volcano, Réunion Island, Indian Ocean. *Journal of Volcanology and Geothermal Research* 13, 131-46.
- HANSON, G. N. 1978. The application of trace elements to petrogenesis of igneous rocks of granitic composition. *Earth and Planetary Science Letters* 38, 26-43.
- HILDRETH, E. W. 1977. *The magma chamber of the Bishop Tuff: Gradients in temperature, pressure and composition*. Ph.D. thesis, University of California, Berkeley.
- HILDRETH, E. W. 1979. The Bishop Tuff: Evidence for the origin of compositional zoning in silicic magma chambers. *Geological Society of America, Special Papers no. 180*, 43-75.
- HILDRETH, E. W. 1981. Gradients in silicic magma chambers: implications for lithospheric magmatism. *Journal of Geophysical Research* 86, 10153-92.
- HILDRETH, E. W. & MAHOOD, G. A. 1982. Large partition coefficients for trace elements in high SiO_2 rhyolites. *Geochimica et Cosmochimica Acta* 47, 11-30.
- KELLER, J. 1981. Quaternary tephrochronology in the Mediterranean region. In *Tephra Studies* (ed. S. Self & R. S. J. Sparks), pp. 227-44. Dordrecht: D. Reidel.
- KELLER, J., RYAN, W. B. F., NINKOVICH, D. & ALTHERR, R. 1978. Explosive volcanic activity in the Mediterranean over the past 200000 years as recorded in deep sea sediments. *Geological Society of America Bulletin* 89, 591-604.
- KORRINGA, M. K. 1971. Steeply-dipping welded tuff mantling the walls of the Pantelleria caldera. *Conference on peralkaline acid volcanism, Catania, Abstracts*.
- KORRINGA, M. K. & NOBLE, D. C. 1971. Distribution of Sr and Ba between natural feldspar and igneous melt. *Earth and Planetary Science Letters* 11, 147-51.
- KORRINGA, M. K. & NOBLE, D. C. 1972. Genetic significance of chemical, isotopic and petrographic features of some peralkaline silicic rocks from the island of Pantelleria. *Earth and Planetary Science Letters* 17, 258-62.
- LEONI, L. & SAITTA, M. 1976. X-ray fluorescence analysis of 29 trace elements in rock and mineral standards. *Rendiconti della Società Italiana di Mineralogia e Petrologia* 32, 497-510.
- MACDONALD, R. 1974. Tectonic setting and magma associations. *Bulletin Volcanologique* 38, 575-93.
- MAHOOD, G. A. 1981. Chemical evolution of a Pleistocene rhyolitic center: Sierra La Primavera, Jalisco, Mexico. *Contributions to Mineralogy and Petrology* 77, 129-49.
- MAHOOD, G. A. & HILDRETH, E. W. 1980. Pantelleria, a new interpretation. *EOS, Transactions of the American Geophysical Union* 61, 1141.
- MASUDA, A., NAKAMURA, N. & TANAKA, T. 1973. Fine structures of mutually normalized rare-earth patterns of chondrites. *Geochimica et Cosmochimica Acta* 37, 239-48.
- MCBIRNEY, A. R. 1980. Mixing and unmixing of magmas. *Journal of Volcanology and Geothermal Research* 7, 357-71.
- MCCORMICK, T. & SHERIDAN, M. F. 1983. Characterization of vapor-phase mineralogy from the green ignimbrite, Pantelleria. In *Microbeam Analysis* (ed. R. Gooley), pp. 39-42. San Francisco Press.
- MICHAEL, P. J. 1983. Chemical differentiation of the Bishop Tuff and other high-silica magmas through crystallization process. *Geology* 11, 31-4.
- NICHOLLS, J. & CARMICHAEL, S. E. 1969. Peralkaline acid liquids. A petrological study. *Contributions to Mineralogy and Petrology* 20, 268-94.
- NOBLE, D. C. & HAFFTY, J. 1969. Minor-element and revised major element contents of some Mediterranean pantellerites and comendites. *Journal of Petrology* 10, 502-9.
- PEARCE, J. A. & CANN, J. R. 1973. Tectonic setting of basic volcanic rocks determined using trace element analyses. *Earth and Planetary Science Letters* 19, 290-300.
- PEARCE, J. A. & NORRY, M. J. 1979. Petrogenetic implications of Ti, Zr, Y and Nb variations in volcanic rocks. *Contributions to Mineralogy and Petrology* 69, 33-47.

- RICCÒ, A. 1882. Terremoti, sollevamenti ed eruzione sottomarina a Pantelleria nella seconda metà di ottobre del 1891. *Bollettino della Società Geografica Italiana* **29**.
- RITTMANN, A. 1967. Studio geovulcanologico e magmatologico dell'isola di Pantelleria. *Rivista Mineraria Siciliana* 106–108, 147–204.
- ROMANO, R. 1968. New petrochemical data of volcanites from the island of Pantelleria (Channel of Sicily). *Geologische Rundschau* **57** (3), 773–83.
- ROMANO, R. 1969. Sur l'origine de l'excès de sodium (ns) dans certaines laves de l'île de Pantelleria. *Bulletin Volcanologique* **33** (3), 694–700.
- SHAW, H. R. 1970. Trace element fractionation during anatexis. *Geochimica et Cosmochimica Acta* **34**, 237–43.
- SHAW, H. R., SMITH, R. L. & HILDRETH, W. 1976. Thermogravitational mechanisms for chemical variations in zoned magma chambers. *Geological Society of America, Abstracts with Programs* **8**, 1102.
- SMITH, R. L. 1979. Ash-flow magmatism. In *Ash-Flow Tuffs* (eds W. Elston & Chapmin), pp. 5–27. Geological Society of America Special Papers no. 180.
- SPARKS, R. S. J., HUPPERT, H. E. & TURNER, J. S. 1984. The fluid dynamics of evolving magma chambers. *Philosophical Transactions of the Royal Society of London* **A310**, 511–34.
- SPERA, F. J. & CRISP, J. A. 1981. Eruption volume, periodicity and caldera area: relationship and inferences on development of compositional zonation in silicic magma chambers. *Journal of Volcanology and Geothermal Research* **11**, 169–87.
- STEIGER, R. H. & JAGER, E. 1977. Convention on the use of decay constants in geology and cosmochronology. *Earth and Planetary Science Letters* **36**, 359–62.
- STORMER, J. C. & NICHOLLS, J. 1978. XLFAC: a program for the interactive testing of magmatic differentiation models. *Computers & Geosciences* **4** (2), 143–59.
- VILLARI, L. 1968. On the geovulcanological and morphological evolution of an endogenous dome (Pantelleria, Mt. Gelkhamar). *Geologische Rundschau* **57** (3), 784–95.
- VILLARI, L. 1969. On particular ignimbrites of the island of Pantelleria (Channel of Sicily). *Bulletin Volcanologique* **33**, 829–39.
- VILLARI, L. 1970. Studio petrologico di alcuni campioni dei pozzi Bagno della Acqua e Gadir (Isola di Pantelleria). *Rendiconti della Società Italiana di Mineralogia e Petrografia* **26** (1), 353–76.
- VILLARI, L. 1974a. Role of the alkali-feldspars fractionation in the evolution of the Pantelleria peralkaline silicic rocks. *Bulletin Volcanologique* **38** (2), 472–484.
- VILLARI, L. 1974b. The island of Pantelleria. *Bulletin Volcanologique* **38** (3), 680–724.
- WASHINGTON, H. S. 1909. The submarine eruptions of 1831 and 1891 near Pantelleria. *American Journal of Science* **27**, 131–50.
- WASHINGTON, H. S. 1913–1914. The volcanoes and rocks of Pantelleria. *Journal of Geology* **21**, 16–27; **22**, 653–70. 623–713.
- WILLEMANT, B., JEFFEREZIC, H., JORON, J. L., & TREUIL, U. 1981. Distribution coefficients of major and trace elements: fractional crystallization in the alkali basalts series of Chaîne des Puys (Massif Central, France). *Geochimica et Cosmochimica Acta* **45**, 1997–2016.
- WOLFF, J. A. & WRIGHT, J. V. 1981a. Rheomorphism of welded tuffs. *Journal of Volcanology and Geothermal Research* **10**, 13–34.
- WOLFF, J. A. & WRIGHT, J. V. 1981b. Formation of the Green Tuff, Pantelleria. *Bulletin Volcanologique* **44** (4), 681–90.
- WRIGHT, J. V. 1980. Stratigraphy and geology of the welded air-fall tuffs of Pantelleria, Italy. *Geologische Rundschau* **69** (1), 26–91.
- ZIES, E. G. 1960. Chemical analyses of two pantellerites. *Journal of Petrology* **1**, 304–8.
- ZIES, E. G. 1962. A titaniferous basalt from the Island of Pantelleria. *Journal of Petrology* **3**, 177–80.
- ZIES, E. G. 1966. A new analysis of cossyrite from the Island of Pantelleria. *American Mineralogist* **51**, 200–5.